Petroleum Science (2021) 18:939–950
https://doi.org/10.1007/s12182-021-00545-2

ORIGINAL ARTICLE

Truss-type maintenance devices and corresponding pipeline lifting control strategies

Tian-Feng Zhao[1] · Qing-Yuan Zhang[1] · Gui Chu[2]

Received: 8 March 2020 / Accepted: 9 July 2020 / Published online: 6 February 2021

Abstract
For new submarine pipeline maintenance lifting equipment, a specialized analysis model is constructed in this study. A pipeline can be divided into the lifted portion and the touch-down portion that lies on the seabed, and each of these portions can be analyzed separately by converting the continuity conditions at the touch-down points to boundary conditions. The typical two-point sequence secant iterative technique is used to obtain the unknown lifted length and determine pipeline lifting configurations. The BVP4C module in MATLAB software is used to solve this multiple-point boundary value problem issued from first-order differential equations. Also, the triple-point lifting mode of truncated maintenance and the two-point lifting mode of online maintenance are discussed. When the lifted heights at truss positions are shown, the lifting deformation, lifting forces, bending moment distribution, and axial force distribution can be analyzed using a dedicated analysis program. Numerical results can then be used to design a lifting strategy to protect the pipeline.

Keywords Pipeline lifting · Multiple-point boundary value · Shooting method · Coulomb friction · BVP4C module

1 Introduction

Submarine pipelines have been widely used to transport oil and gas, from offshore oil and gas fields to storage facilities and processing terminals onshore. When laying submarine pipelines and while they are in service, a pipeline lying on a seabed may be lifted to a barge deck for welding to repair mechanical damage or even replace local segments, which usually includes four steps: (1) underwater dredging, cutting and removing the damaged pipe section, connecting the ship's sling at the pipe cut positions, and having divers arrange buoys or float bags along the pipe segment to be raised; (2) lifting the cut pipelines to the deck and lowering the pipelines back to the seabed after welding the flanges; (3) connecting the cuts of both sides of the pipeline with a new pipe segment using a ball flange to replace the damaged pipeline section; and (4) trenching with a hydraulic trenching machine to sink the repaired pipeline back into the trench.

During these repair procedures, divers arrange buoys or float bags along the pipeline to reduce stress on the submarine pipeline during lifting to avoid damaging the pipeline. However, bundling buoys or float bags typically requires a long time, particularly when a long pipe section must be lifted from a relatively deep seabed with many buoys or float bags. Additionally, dredging before maintenance and trenching the pipeline after maintenance currently requires using a hydraulic jet trencher, and the substitution of these pieces of equipment or ships during construction also reduces the efficiency of pipeline maintenance.

Recently, new submarine pipeline maintenance equipment has been proposed. This equipment has a pair of slide rails arranged on both sides of the moon pool on the platform deck, and two truss frames arranged on the slide rails, which guide two lifting trusses, thus allowing convenient locating at a designated position to lower the lifting trusses to the sea floor to lift the pipe. The lifting truss is composed of several truss single sections, and each truss section is connected by a holding card device, which can adjust the connection between the truss sections and switch between a fixed and hinged connection. Therefore, the platform can fold the lifting truss to ensure the safety

Edited by Xiu-Qiu Peng and Chun-Yan Tang

✉ Qing-Yuan Zhang
zh_qingyuan@163.com

[1] College of Safety and Ocean Engineering, China University of Petroleum-Beijing, Beijing 102249, China

[2] China Huanqiu Contracting and Engineering (Beijing) CO., Ltd., Beijing 100012, China

of navigation when driving but can also adjust the lifting truss to be straight to meet the lifting requirement of the water depth.

Based on working conditions, the pipe puller and dredging equipment are connected at the bottom of the lifting trusses. The pipe puller is used to grasp the submarine pipeline, and the dredging equipment is used to remove sludge before the pipe is lifted and to sink the pipeline after repairs are complete. A crane with a sling is located on the platform deck, and a through groove with a rotatable support is arranged at a lower portion of the lifting truss near the crane sling. The integrated arrangement of this submarine pipeline maintenance equipment and the structural details of the dredging equipment and pipe puller are shown in Fig. 1.

Under typical working conditions, a three-point lifting mechanism for a submarine pipeline consists of a crane sling, support, and pipe puller. Because three-point lifting is beneficial to the pipeline, the operation of the buoy or float bag is not required. A reel is placed on the deck of the platform so that the salvaged subsea pipeline can be wound onto a reel for recycling or for laying flexible pipes or cables. To optimize the application of this maintenance system, it is important to consider the lifted height, spacing between the sling and two trusses, internal forces in the pipeline, and environmental effects. In addition to a reasonable pipe configuration, corresponding truss lifting strategies must also be planned.

Hobbs (1979) performed pioneering work on the theoretical study of the mechanical behavior of lifting pipelines. Assuming that the seabed is completely rigid, he studied lift forces during the two-point lifting process with and without axial force using small deformation beam theory. Later, using large deformation beam theory, Xing et al. (2002) investigated the single-sling lifting process from a rigid seabed. They converted the moving boundary problem to a two-point boundary value problem using a varied arc dimensionless transformation and obtained a numerical solution to the problem with the shooting method. Zeng et al. (2013) established three models and numerically solved the same problem, combining the second- or third-order differential equations with different boundary conditions. Xiong et al. (2010) presented a two-point lifting scheme and solved the problem using the shooting method to reduce the possible excessive moment subjected during single-point lifting. Lun et al. (2013) established a finite element model based on engineering practices of the picking-up and laying-down processes of submarine pipelines, by which he studied the configuration and stress distribution of the pipeline acted upon by a longitudinal current, lateral current and seabed friction. Li et al. (2014) established a calculation model for

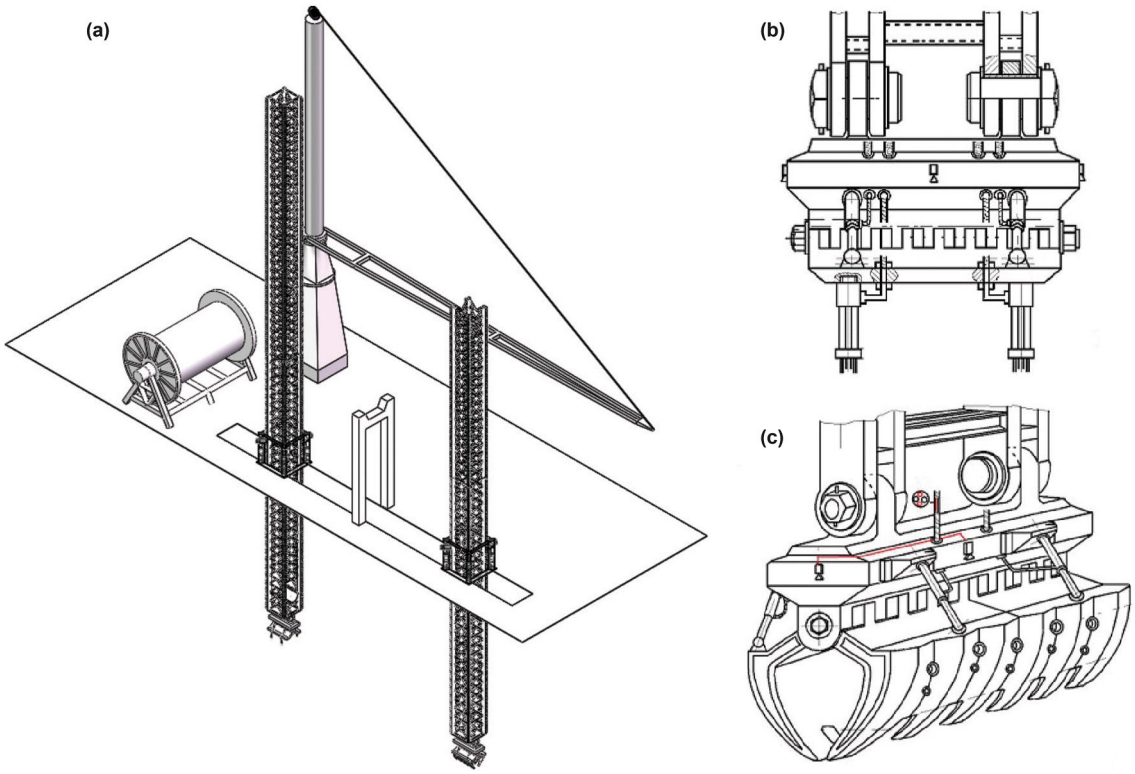

Fig. 1 Integrated arrangement of new submarine pipeline maintenance equipment: **a** lifting trusses in the moon pool; **b** dredging equipment; and **c** pipe puller

the butting and sinking of offshore pipelines, and performed comparative analyses on the pipeline morphology, bending moment distribution, and stress state of the pipeline for different sinking schemes. Using OrcaFlex software, Bian et al. (2015) studied the lifting process of a horizontal subsea buried pipeline.

Wang et al. (2015) investigated the transfer process during the installation of a steel lazy-wave riser (SLWR) and proposed a comprehensive mechanical model based on the nonlinear large deflection beam theory for the deep-water riser transfer process. This model can analyze the length and tension of the two cables used to lift the riser's pull-head: A&R cable of the installation vessel and the pull-in cable of the production platform. Liu et al. (2016) studied pipeline lifting during horizontal directional drilling engineering and described stress variations in the pipeline during lifting using a verified finite element model. This study indicates that a double gondola lifting operation can significantly reduce pipeline stress by approximately 20%. Oh et al. (2020) developed a simulation-based design framework for the shape design of the SLWR using open-source-based process integration and design optimization (PIDO) software and found the optimal shape for the installation process of a SLWR. Hong and Liu (2020) analyzed the features of lifting deformation in a pipeline laid on a seabed sleeper. Based on the nonlinear relationship between the lifting displacement and temperature difference, three key points and four relevant key parameters that describe the lifting displacement curve were proposed and calculated for the conditions of a pipeline with different combinations of influential factors.

However, existing lifting models cannot satisfy the application requirements of new submarine pipeline maintenance equipment, which requires clarity of the effects of the lifted height, seabed resistance, and spacing between lifting points on the pipeline to develop available pipe lifting schemes. Therefore, this paper presents a rational mechanical model to investigate the effects of these factors and concurrently provides support for the use of this new maintenance device. In this model, the pipeline being lifted is divided into the lifted portion and the touch-down portion that lies on the seabed. Because the bending curvature of the lifted portion is large, large deformation extensible beam theory is used to analyze the lifting process. For the touch-down portion, the axial interaction between the pipeline and the rigid seabed is assumed to follow the Coulomb friction rule, and based on whether the pipeline slips on the seabed, the static or sliding friction force is defined.

The touch-down point is considered to be the boundary of the lifted pipe segment, and a first-order differential equation with a multiple-point boundary value can be used to describe the deformation of this pipe segment. Because the length of this pipe segment is unknown, and whether the pipeline slips on the rigid seabed also cannot be determined a priori, the two-point sequence secant method is used to iteratively solve for the lifted length and movement of the pipeline. In this paper, the solution to this problem is obtained using the built-in BVP4C module of MATLAB software.

2 Mechanical model and analytical solution

2.1 Fundamental assumptions

In practical applications, the arrangement of the lifting points, the variable environmental loads, the resistance from the seabed, and water depth directly influence the lifting forces and internal forces in a pipe segment. These factors involve many engineering data, some even random data, making it difficult to resolve the situation comprehensively; thus, the following assumptions are made to facilitate the analysis:

- The pipeline is lifted by two or three lifting points, and the lifted heights are specified at these points;
- The in-plane current is uniform in the axial direction of the pipeline, and the wave load is negligible;
- The seabed is simplified to be horizontal and flat, and the axial interaction between the pipe and the rigid seabed is consistent with the Coulomb friction rule;
- The shear deformation of the pipeline is not considere;
- The stiffness influences of the girth welds between simple roots are ignored;
- The analysis is restricted to the quasi-static planar case.

The Cartesian coordinate system is built with its origin selected at the touch-down point, and its x-axis is along the seabed. The geometric configuration of the pipeline during the three-point lifting operation is shown in Fig. 2.

2.2 Fundamental equations

To perform a mechanical analysis, the pipeline is divided into the lifted portion and the touch-down portion. The governing

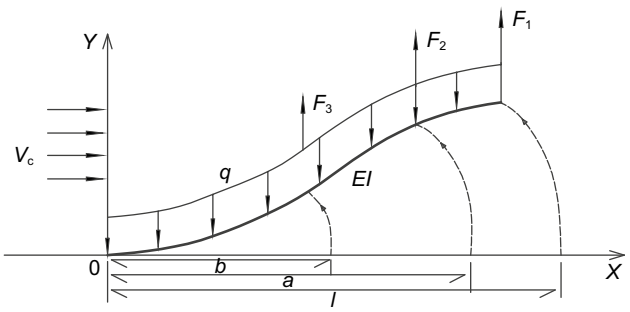

Fig. 2 Geometric schematic diagram of the lifted pipeline

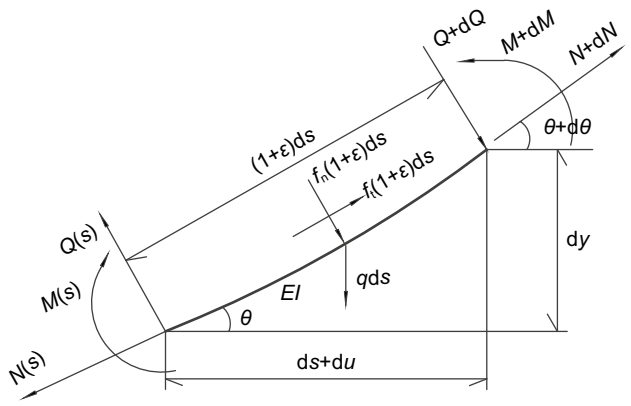

Fig. 3 Internal forces acting on the differential element of the lifted pipe segment

equations can be obtained by considering the equilibrium of the differential element, geometric relation, and physical relation.

2.2.1 Lifted portion

Under external loads, the differential element of the lifted pipe segment is shown in Fig. 3, where $\theta(s), \theta(s) + \mathrm{d}\theta(s)$ are the rotation angles of the deformed differential element with the axial force $N(s)$, bending moment $M(s)$, and shear force $Q(s)$, which are all single value functions of arc length s. The internal forces on the right section of this deformed differential element are $N + \mathrm{d}N$, $M + \mathrm{d}M$, and $Q + \mathrm{d}Q$. Considering the equilibrium of this differential element, the following differential equations can be obtained by neglecting the second-order infinitesimal terms because $\mathrm{d}s$ approaches zero, $\cos(\mathrm{d}\theta) \approx 1$, and $\sin(\mathrm{d}\theta) \approx \mathrm{d}\theta$:

$$-q\mathrm{d}s \cdot \sin\theta + \mathrm{d}N + Q\mathrm{d}\theta + f_\mathrm{t}(1+\varepsilon)\mathrm{d}s = 0 \tag{1}$$

$$-q\mathrm{d}s \cdot \cos\theta - \mathrm{d}Q + N\mathrm{d}\theta - f_\mathrm{n}(1+\varepsilon)\mathrm{d}s = 0 \tag{2}$$

$$\mathrm{d}M - Q(1+\varepsilon)\mathrm{d}s = 0 \tag{3}$$

$$f_\mathrm{n} = 0.5\rho_\mathrm{w}c_\mathrm{n}D\left|v_\mathrm{c}\sin\theta\right|v_\mathrm{c}\sin\theta \tag{4}$$

$$f_\mathrm{t} = 0.5\rho_\mathrm{w}c_\mathrm{t}D\left|v_\mathrm{c}\cos\theta\right|v_\mathrm{c}\cos\theta \tag{5}$$

$$N = EA\varepsilon \tag{6}$$

where f_n and f_t are hydrodynamic forces per unit length in the normal and tangential directions; C_n and C_t are coefficients of the hydrodynamic forces; ρ_w is the density of sea water; v_c is the current speed; D is the outer diameter of the pipe; E is the elastic module of the pipe material; A is the cross-sectional area of the pipe; and ε is the axial strain of the pipe.

Because the bending deformation is large, and the pipeline may be considered to be a slender member, the relation between curvature and bending moment is:

$$\frac{\mathrm{d}\theta}{\mathrm{d}s} = \frac{M(s)}{EI}(1+\varepsilon) \tag{7}$$

For a large deformation slender beam, the differential relation between the rotation and deflection is:

$$(1+\varepsilon)\sin\theta = \frac{\mathrm{d}y}{\mathrm{d}s} \tag{8}$$

$$(1+\varepsilon)\cos\theta = \frac{\mathrm{d}u}{\mathrm{d}s} + 1 \tag{9}$$

where $y(s)$ and $u(s)$ are the deflection and horizontal displacement at a point on the pipe axis, respectively.

The horizontal component of the external loads for the lifted part is:

$$N_0 = \int_0^l \left(f_\mathrm{t}\cos\theta + f_\mathrm{n}\sin\theta\right)(1+\varepsilon)\mathrm{d}s \tag{10}$$

2.2.2 Touch-down portion

The touch-down portion of the pipeline behaves like an axially stiff beam due to the horizontal external loads from the lifted portion. If the pipe does not slip on the seabed, the horizontal displacement of the touch-down point is zero when the axial force is below the concentrated static friction force F_c resulting from the concentrated reaction R_0 at this point based on the Coulomb frictional rule.

Otherwise, a certain length L_s of the pipe will slip on the seabed, and the axial distribution of the frictional force should be considered. The frictional force is assumed to act

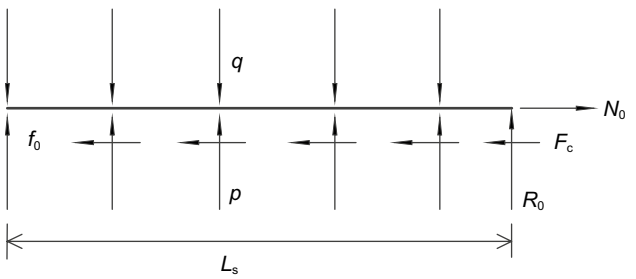

Fig. 4 Forces acting on the differential element of the touch-down portion of the pipe

on the length L_s of the pipe uniformly, and the magnitude is $f_0 = q\mu$, as shown in Fig. 4.

The governing differential equation for the slipping situation can be obtained straightforward by considering the equilibrium of the differential element:

$$\mathrm{d}N - f_0 \mathrm{d}x = 0 \tag{11}$$

where f_0 is the seabed friction per unit length of the pipeline. Note that $x = -L_s$, $N = 0$, and the axial force can be expressed explicitly as:

$$N = f_0\left(x + L_s\right) \tag{12}$$

The resulting axial strain is:

$$\varepsilon = \mathrm{d}u/\mathrm{d}x = N/EA \tag{13}$$

Note that $x = -L_s$, $u = 0$, and integrating Eq. (13), the axial displacement can be expressed as:

$$u = f_0\left(x + L_s\right)^2/2EA \tag{14}$$

Due to the concentrated friction force F_c resulting from the reaction R_0 at the touch-down point, the axial force at this point is:

$$N_0 = f_0 \cdot L_s + \mu R_0 \tag{15}$$

where μ is the friction coefficient between the pipe and the seabed.

2.3 Boundary and continuity conditions

The natural coordinate s of the touch-down point is equal to zero, and the deflection, rotation angle, and bending moment of this pipe point are all zero. The horizontal displacement and the axial force of this point can be expressed by Eq. (16d) and (16e):

$$y(0) = 0 \tag{16a}$$

$$y'(0) = 0 \tag{16b}$$

$$M(0) = 0 \tag{16c}$$

$$u(0) = 0 \ (\text{or } \ u(0) = f_0 L_s^2/2EA) \tag{16d}$$

$$N(0) = N_0\left(\text{or } \ N(0) = \mu R_0 + f_0 L_s\right) \tag{16e}$$

where the quantity in parentheses corresponds to the slipping situation.

Corresponding to the online repair operations of subsea pipelines, the lift height δ_3 is known, and the rotation angle and shear force in the middle of the lifted section (i.e., $s = l$) are zero when the two-point lifting mode is used at one of two lifting positions (i.e., $s = b$). Thus,

$$y(b) = \delta_3 \tag{17a}$$

$$y'(l) = 0 \tag{17b}$$

$$Q(l) = 0 \tag{17c}$$

Corresponding to the truncation repair or the recycling of abandoned subsea pipelines, the lift heights are known, and the bending moment at the truncation point is zero when the triple-point lifting mode is used at three lifting points (i.e.,$s = l$, $s = a$ and $s = b$). Thus,

$$y(l) = \delta_1 \tag{17d}$$

$$M(l) = 0 \tag{17e}$$

The initial natural coordinate of the second lifting point is $s=a$, where the deflection, rotation angle, bending moment, axial displacement, and axial force should be continuous. Thus:

$$y(a) = \delta_2 \tag{18a}$$

$$y(a^-) = y\left(a^+\right) \tag{18b}$$

$$y'(a^-) = y'\left(a^+\right) \tag{18c}$$

$$M(a^-) = M\left(a^+\right) \tag{18d}$$

$$u(a^-) = u\left(a^+\right) \tag{18e}$$

$$N(a^-) = N\left(a^+\right) \tag{18f}$$

$$\begin{array}{l} Q(a^-) + F_N \cdot \cos\theta - Q\left(a^+\right) = 0 \\ N(a^-) - F_N \cdot \sin\theta - N\left(a^+\right) = 0. \text{ That is} \end{array} ,$$

$$\left[Q\left(a^+\right) - Q(a^-)\right] \cdot \tan\theta = N(a^-) - N\left(a^+\right) \tag{18g}$$

The initial natural coordinate of the third lifting point is $s = b$, where the deflection, rotation angle, bending moment, axial displacement, and axial force should be continuous. Thus,

$$y(b) = \delta_3 \tag{18h}$$

$$y(b^-) = y\left(b^+\right) \tag{18i}$$

$$y'(b^-) = y'\left(b^+\right) \tag{18j}$$

$$M(b^-) = M(b^+) \tag{18k}$$

$$u(b^-) = u(b^+) \tag{18l}$$

$$\begin{aligned} &Q(b^-) + F_N \cdot \cos\theta - Q(b^+) = 0 \\ &N(b^-) - F_N \cdot \sin\theta - N(b^+) = 0. \text{ That is} \end{aligned} ,$$

$$\left[Q(b^+) - Q(b^-)\right] \cdot \tan\theta = N(b^-) - N(b^+) \tag{18m}$$

2.4 Solution processes

2.4.1 Length of the lifted portion

Equations (1)–(3), (7)–(9) are the six governing differential equations for the lifted portion of the pipeline, which include six unknowns (N, Q, M, u, y, and θ). The boundary conditions include Eqs. (16) and (17), and the continuity condition is Eq. (18). Together with Eq. (10), which yields the horizontal component of the external loads, there are exact equations to determine all unknowns. Therefore, the lifted arc length l and the axial force N_0 at the touch-down point (or slipping length L_s) as well as the solution can be obtained.

Because the touch-down point from the seabed is undetermined, the total lifted length l is an element of the solution, and the total lifted length must be determined iteratively when solving. In this study, the lifted height δ and axial force N_0 at the touch-down point (or slipping length L_s) are considered to be additional conditions, and iterative calculations are made by the two-point sequence secant method by revising the lifted length l and axial force N_0(or L_s) until the calculated results meet the precision requirement. Then, the lifted arc length can be obtained and whether the pipe slips on the seabed can be determined.

2.4.2 Solution flow chart for the boundary value problem

The built-in BVP4C module is used to solve this first-order differential equation by considering the requirements of the calculation precision and the rate of convergence. The continuity conditions at the touch-down point are transformed into boundary conditions of the lifted portion of the pipe. The associated displacement and internal forces can be obtained by solving the multiple-point boundary value problem. The flow chart of the solution can be given as follows:

1. Input EI,EA, q, δ, μ, v_c, etc.;
2. Assume two sets of different initial values $x_i^{(k-1)}$ and $x_i^{(k)}$ $(i = 1, 2)$; if the pipe does not slip on the seabed, $x = \left[L, N_0\right]^T$; otherwise,$x = \left[L, L_s\right]^T$ (k is the number of iterations);
3. Solve the multiple-point boundary value problem using the BVP4C module and obtain $f\left(x^{(k)}\right)$, where $f_1\left(x^{(k)}\right)$ is the calculated lift height and $f_2\left(x^{(k)}\right)$ is the calculated total horizontal force of the lifted part.
4. Calculate $h_j^{(k)} = x_j^{(k-1)} - x_j^{(k)}$, $x^{(k)} + h_j^{(k)} e_j$ and $f\left(x^{(k)} + h_j^{(k)} e_j\right)(j = 1, 2)$, where $e_j^T = \{0, 1, 0\}$ (the element in column j is 1, and the other elements are 0).
5. Compute the matrix $H^{(k)} = \left[\left(f\left(x^{(k)} + h_1^{(k)} e_1\right) - f\left(x^{(k)}\right)\right)/h_1^{(k)}, \left(f\left(x^{(k)} + h_2^{(k)} e_2\right) - f\left(x^{(k)}\right)\right)/h_2^{(k)}\right]$.
6. Compute the new x, i.e., $x^{(k+1)} = x^{(k)} - \left[H^{(k)}\right]^{-1} f\left(x^{(k)}\right)$.
7. If $\left|\left(x_i^{(k+1)} - x_i^{(k)}\right)/x_i^{(k)}\right| > eps (i = 1, 2)$, let $x^{(k-1)} = x^{(k)}, x^{(k)} = x^{(k+1)}, f\left(x^{(k)}\right) = f\left(x^{(k+1)}\right)$, return to step (4) ($eps$ is the allowance).
8. Otherwise, the iterative process is terminated. $f\left(x^{(k+1)}\right)$ is obtained using the BVP4C module; thus, the lifted length and the associated solution are obtained.
9. Check whether the assumed slipping or no-slipping condition is met.

2.5 Validation checks

Three CNOOC subsea pipeline datasets are investigated to validate the feasibility of the proposed lifting calculations and the applicability of this truss-type maintenance device. The pipeline specification data are shown in Table 1.

Ignoring horizontal forces and only considering the vertical balance of the pipeline during lifting, Figs. 5 and 6 show the lifting configurations and bending moment distributions of three CNOOC pipelines under triple-point lifted heights when the crane hoisting point and two lifting trusses are

Table 1 CNOOC pipeline specification data

Pipeline	O.D., mm	W.T., mm	A, m^2	I, m^4	EI, MN m^2	Submerged weight*, N/m
BZ28-2S WHPB to BZ34-24 CEPA	168.3	12.7	6.208159e^{-3}	1.891366e^{-5}	3.9719	482.45
BZ35-2 CEPA to BZ29-4 WHPC	273.1	14.3	1.162652e^{-2}	9.763653e^{-5}	20.50367	900.82
BYT WHPA to HY1-1 CEP	355.6	14.3	1.533281e^{-2}	2.236486e^{-4}	46.966	1189.0

*The pipeline in this study is empty when undergoing maintenance, and the submerged weight is only the weight of the steel pipe in sea water

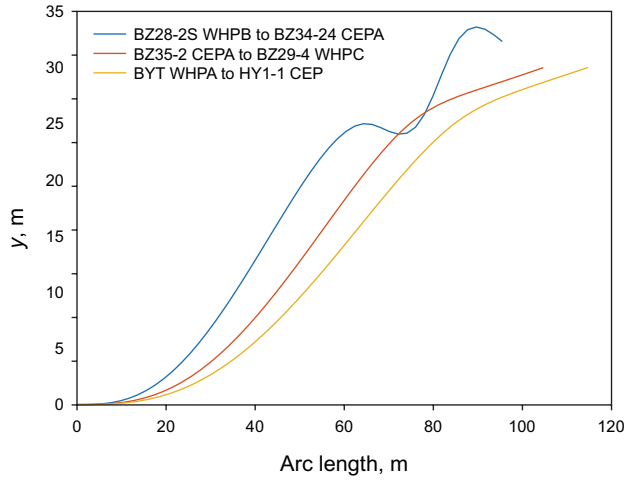

Fig. 5 Lifting configurations of three CNOOC pipelines under triple-point lifted heights ($\delta_1 = 30$, $\delta_2 = 28$ and $\delta_3 = 25$ m)

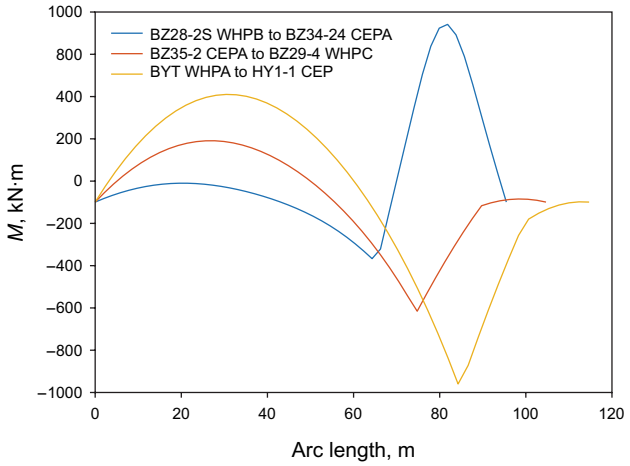

Fig. 6 Bending moment distributions of three CNOOC pipelines under triple-point lifted heights ($\delta_1 = 30$m, $\delta_2 = 28$m and $\delta_3 = 25$m)

lifted by 30 m, 38 and 25 m, respectively. When the bending stiffness of the pipeline is relatively small, a more complex lifting configuration may appear under triple-point lifting, such as that of the BZ28-2S WHPB pipeline. However, the proposed algorithm can still be used to analyze the bending moment distribution of the lifted pipeline in this case to judge whether lifting is feasible.

3 Application analyses

To demonstrate the potential of the proposed truss-type maintenance device, one large-diameter thick-walled submarine pipeline is investigated as an example, and the specification data of this pipeline are listed in Table 2. Because the purpose of this analysis is to evaluate the device's capability rather than the complex movement of the pipeline, only the vertical lifting direction is analyzed here; thus, the effects of waves, currents, and seabed frictions are ignored. The operating modes of triple-point and two-point lifting are analyzed for this new type of submarine pipeline lifting device.

Table 2 Specification data of the example pipeline (Lenci and Callegari 2005)

Outer diameter, D	609.6 mm
Wall thickness, t	31.8 mm
Young's Module, E	210 GPa
Pipe section area, A	5.77237 E^{-2} m^2
Pipe second moment of area, I	2.416199 E^{-3} m^4
Submerged weight of the pipe per unit length, q	3.8666 kN/m
Allowable bending moment, M	2959 kN·m (Safety Factor 1.2)
Allowable axial force, N	21,550 kN (Safety Factor 1.2)
Density of the sea water, ρ_w	1025 kg/m^3

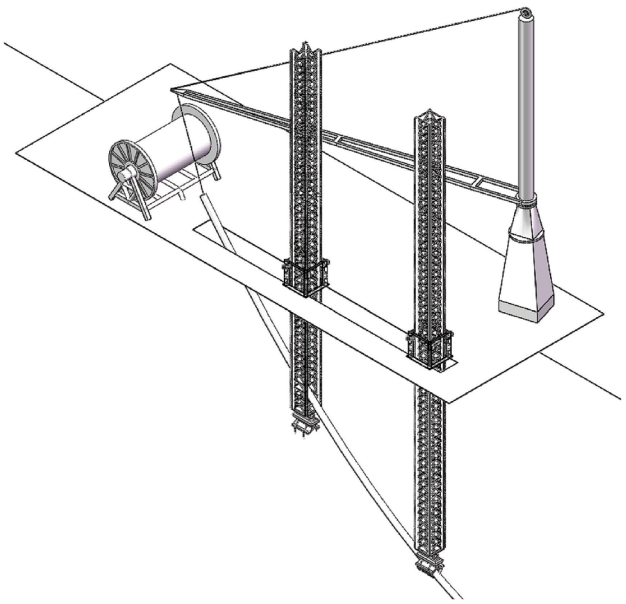

Fig. 7 Layout of the triple-point lifting operation

3.1 Triple-point lifting

For the maintenance or recycling of submarine pipelines, the layout of the triple-point lifting operation is shown in Fig. 7. During lifting, the lifted heights δ_1, δ_2, and δ_3 of the crane hoisting point and two lifting trusses determine the deformation and internal force of the pipeline. Given a series of lifted heights, the corresponding maximum bending moments, minimum bending moments, and

Table 3 Maximum bending moments, minimum bending moments and lifting forces during triple-point lifting

δ			F			M	
δ_1, m	δ_2, m	δ_3, m	F_1, kN	F_2, kN	F_3, kN	M_{max} (δ_2), kN·m	M_{min} (δ_3), kN·m
5.0	4.0	3.0	40.58	− 40.37	251.62	211.6	− 1093
8.0	7.0	6.0	65.90	− 191.96	424.44	530.4	− 2533
12.0	9.7	8.0	204.94	− 467.73	568.76	2405	− 2491

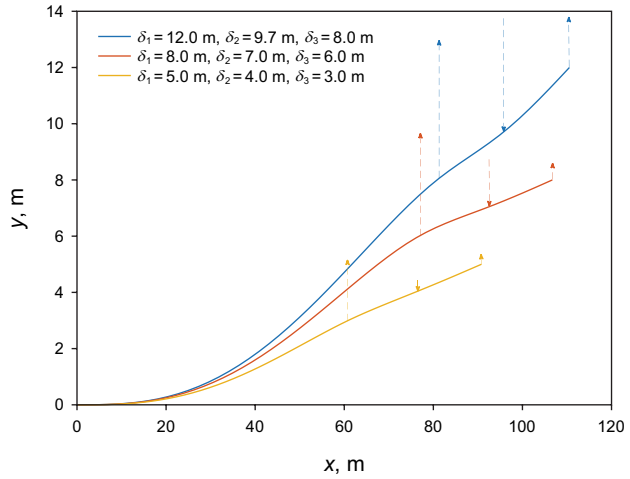

Fig. 8 Lifting deformations for different series of triple-point lifted heights

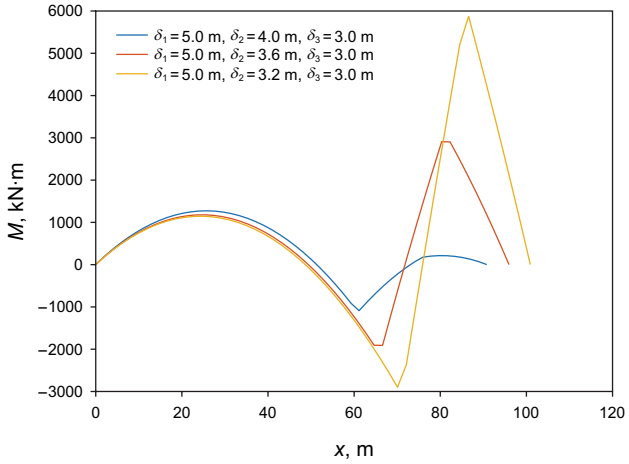

Fig. 9 Bending moment distribution when the lifted heights of the crane hoist point and the second lifting truss are 5 and 3 m, respectively

lifting forces are shown in Table 3. During the analyses, the horizontal space between the crane hoisting point and the first lifting truss and that between two lifting trusses are both set to 15 m.

For three series of lifted heights, Fig. 8 shows the lifting deformations of the pipeline and proportionally indicates the lifting loads with dashed arrows. For the triple-point lifting mode, the crane hoisting point and the second lifting truss exert upward pulling forces, while the first lifting truss applies a downward force.

In practical engineering, the vertical displacements of the three lifting points are control parameters, and unfavorable lifted height combinations at the three positions may cause excessive bending in the lifting position. Figures 9, 10 and 11 compare the differences in bending moment distributions along the pipeline when the lifted heights of the first truss (δ_2) change. These results indicate that when the lifted heights of the first truss closely follow those of the crane hoisting point, acceptable blue bending moment distributions are induced. Once the lifted heights of the first truss significantly lagged behind the crane hoisting point, unacceptable yellow bending moment distributions may be

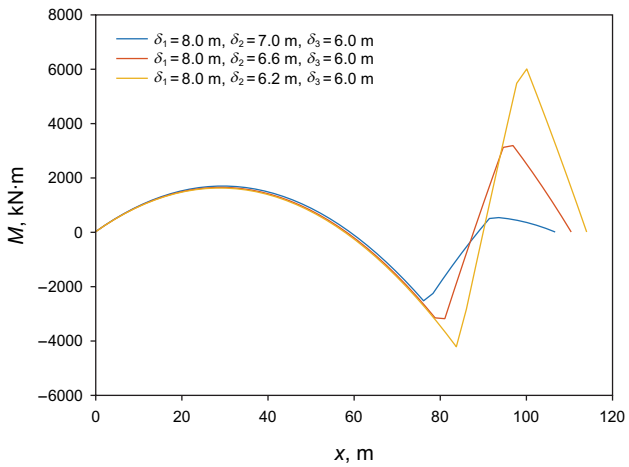

Fig. 10 Bending moment distribution when the lifted heights of the crane hoist point and the second lifting truss are 8 and 6 m, respectively

induced, while two truss lifting positions may experience overbending.

For the recycling operations of the abandoned pipelines, the red bending moment distributions are acceptable for this

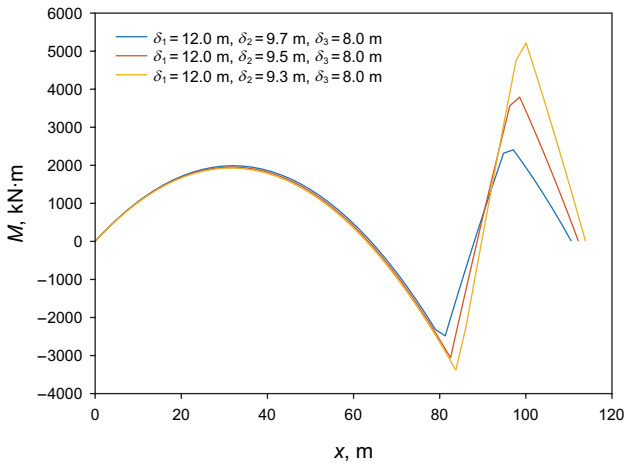

Fig. 11 Bending moment distribution when the lifted heights of the crane hoist point and the second lifting truss are 12 and 8 m, respectively

example pipeline; thus, the peaks of the bending moments are near the limit of pipe bending.

3.2 Two-point lifting

In some cases, it is necessary to perform pipeline online maintenance; thus, the two-point lifting mode in shallow water can be used, as shown in Fig. 12. Based on the analysis model described above, two lifting trusses exert vertical lifting forces, whose functions are similar to the second lifting truss in the triple-point mode.

Based on the assumption that the two lifting trusses are 30 m apart, the lifting deformations for the two-point lifting mode can be analyzed when the lifted heights of two trusses are given. Figure 13 shows the lifting deformations of the example pipeline when two lifted heights increase from 3.0 to 4.5 m.

Table 4 shows the lifting forces and maximum bending moments at two lifting positions for four lifted heights, the maximum axial force in the overhanging sections on

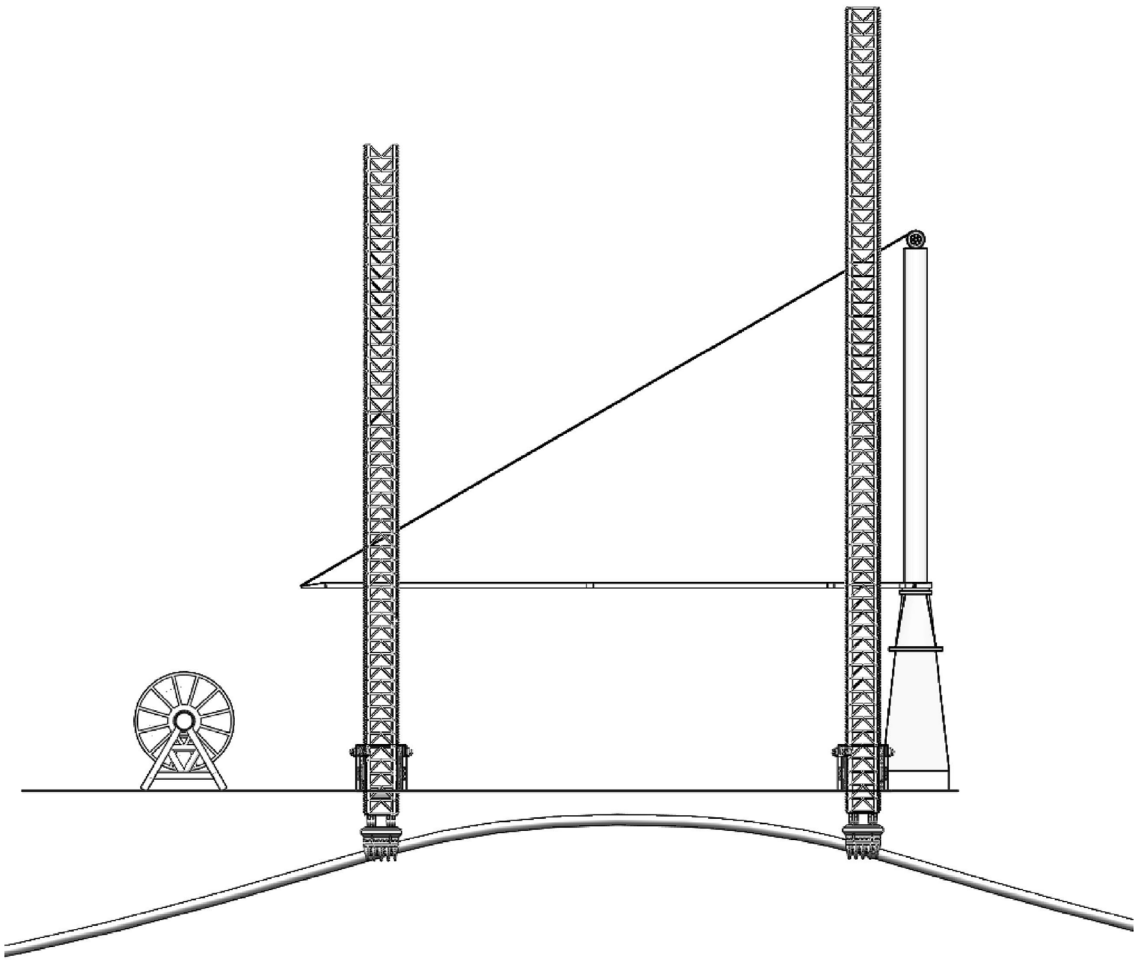

Fig. 12 Layout of the two-point lifting operation

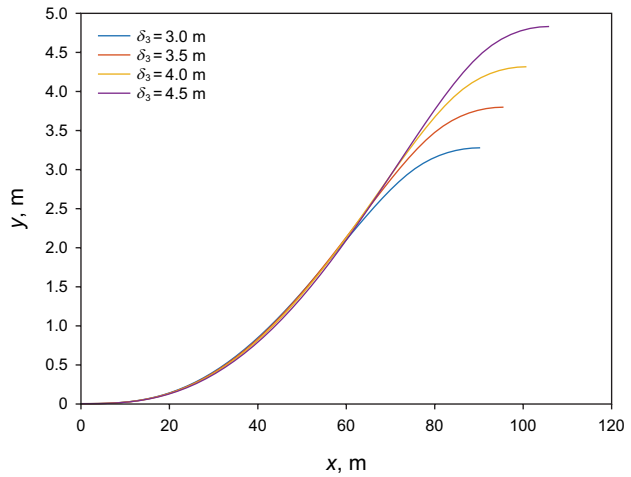

Fig. 13 Lifting deformations for the two-point lifting mode (one side)

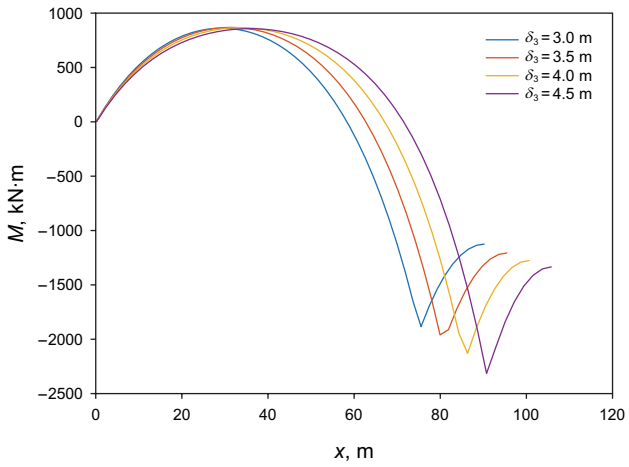

Fig. 14 Bending moment distribution for the two-point lifting mode (one side)

both sides, and the results at the vertex of the entire lifted segment, including the lifted heights, bending moments, and axial forces. The relations between the bending moment M and the position x are shown in Fig. 14. The overhanging sections and the section in the moonpool exhibit convex parabolic-shaped bending moment distributions, and the lifting position yields the largest negative bending moment.

3.3 Effects of the lifting truss spacing

Figure 15 contrasts the bending moment distributions for different truss spacings under the two-point lifting mode and shows that the lifting truss spacing primarily influences the bending moment of the pipeline segment in the moonpool. Figure 16 shows the axial force distributions of the lifted pipeline and indicates that the maximum axial force exists in the pipeline section before the lifting truss and marginally increases when the truss spacing increases from 24 to 36 m.

In the triple-point lifting mode, Fig. 17 compares the distribution of pipeline bending moments when the two lifting trusses have intervals of 15, 18, or 20 m, and

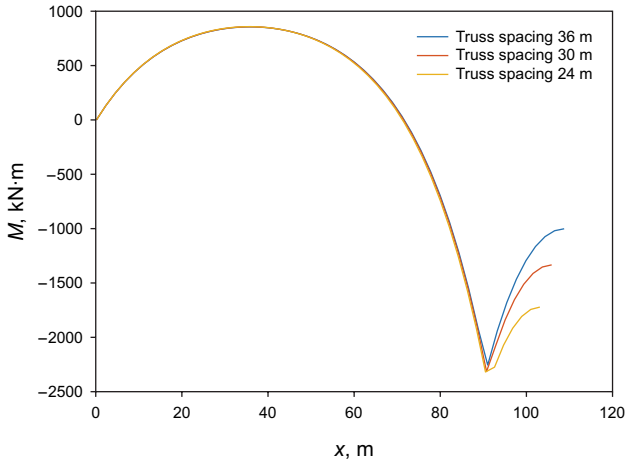

Fig. 15 Bending moment distribution for different truss spacings (two-point lifting mode, one side, 4.5 m lifted height at truss positions)

comparison confirms the feasibility of a 15 m interval. Figure 18 compares the corresponding axial force distributions.

Table 4 Lifting forces, bending moments, and axial forces during two-point lifting

Two lifting positions			The overhanging segments	The vertex of the entire lifting segment		
δ_3, m	F_3, kN	$M_{max}(\delta_3)$, kN·m	N_{max}, kN	δ_0, m	M_0, kN·m	N_0, kN
3.0	279.5	− 1912	1281.0	3.27	− 1124.4	1271.6
3.5	301.5	− 2066	1440.6	3.79	− 1205.4	1429.6
4.0	323.1	− 2207.9	1592.4	4.31	− 1274.2	1579.7
4.5	344.6	− 2339.1	1737.3	4.83	− 1333.4	1722.9

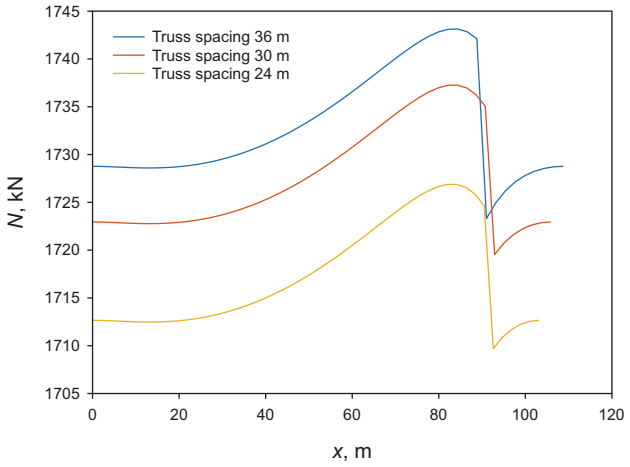

Fig. 16 Axial force distribution for different truss spacings (two-point lifting mode, one side, 4.5 m lifted height at truss positions)

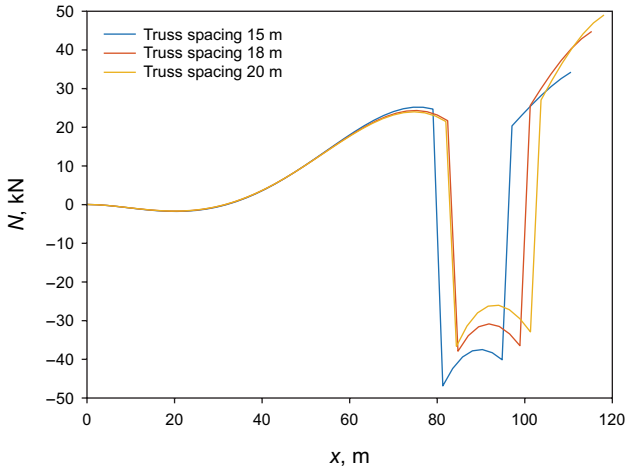

Fig. 18 Axial force distribution for different truss spacings (triple-point lifting mode, $\delta_1 = 12$, $\delta_2 = 9.7$, $\delta_3 = 8$ m)

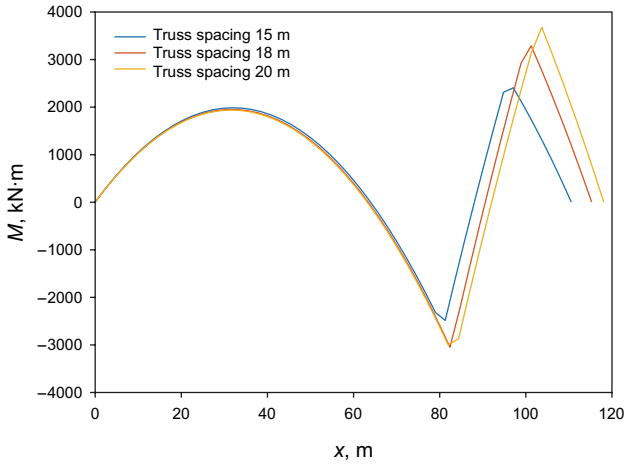

Fig. 17 Bending moment distribution for different truss spacings (triple-point lifting mode, $\delta_1 = 12$, $\delta_2 = 9.7$, $\delta_3 = 8$ m)

4 Conclusions

The proposed truss-type lifting device can simplify pipeline lifting and be easily combined with dredging and trenching devices to improve pipeline maintenance efficiency. During lifting, the pipeline is partially suspended after one end is raised, which leaves the overhanging segment long, and the bending deformation large, resulting in a considerable bending moment and axial force in the pipeline; thus, a suitable pipeline lifting control strategy must be developed.

Based on the proposed mechanical model, fundamental equations, and special boundary conditions, a set of numerical analysis methods is developed in this study when the vertical deflection, rotation angle, bending moment, shear force, horizontal displacement, and axial force can be determined for each section of the lifted pipeline.

In this study, a large-diameter pipeline is used as an example to investigate the practicability of the two-point and triple-point lifting modes. Comparative analyses on different lifted height combinations are also performed and indicate the following lifting strategies.

During triple-point lifting, the lifted height combination (δ_1, δ_2, δ_3) is the critical factor that dominates the lifting configuration and internal forces of the pipeline. The crane hoisting point (δ_1) and the second lifting truss (δ_3) exert upward pulling forces, while the first lifting truss (δ_2) applies a downward force. As the lifted height increases, the load of each lifting point and the bending moment at the lifting point increase rapidly. To decrease the peak bending moments, the lifted height of the first truss (δ_2) must closely follow that of the crane hoisting point (δ_1) instead of approaching that of the second truss (δ_3). The spacing of the two trusses also influences the peak bending moments at the two truss lifting points. When the spacing increases from 15 to 20 m for the same lifted heights, the peak bending moments increase beyond the allowable value. When the truss spacing increases, the axial force distribution in the overhanging segment remains relatively static. Thus, even though the axial forces in the pipe sections sandwiched between the three lifting points change significantly, the risk of yielding is not involved because the three-point lifting mode typically does not induce significant axial forces.

During two-point lifting, the vertex of the lifted segment rises from 3.27 to 4.83 m as the truss lifting heights increase from 3 to 4.5 m, and the lifting forces and bending moments induced in the lifting positions both increase synchronously. Concurrently, maximum axial forces in the overhanging

segments grow quickly. Therefore, for subsea pipelines, online maintenance lifting can be expected in shallow water only after the bending moment and axial force are evaluated, or only to lift the pipeline to be repaired off the seabed instead of to the deck.

Acknowledgements This paper was financially supported by the National Natural Science Foundation of China (Grant No. 51679251), and the authors would like to express their sincere thanks.

References

Bian DY, Du Y, Liu JF, et al. Analysis on horizontal tube lifting motion of subsea buried pipeline. Ship Eng. 2015;37(12):92–7. https://doi.org/10.13788/j.cnki.cbgc.2015.12.092 (**in Chinese**).

Hobbs RE. The lifting of pipelines for repair or modification. Proc Instn Civ Engrs. 1979;67(1):1003–13. https://doi.org/10.1680/iicep.1979.2787.

Hong ZH, Liu WB (2020) Modelling the vertical lifting deformation for a deep-water pipeline laid on a sleeper. Ocean Eng. 199. https://doi.org/10.1016/j.oceaneng.2020.107042

Oh J, Jung D, Kim H, et al (2020) A study on the simulation-based installation shape design method of steel lazy wave riser (SLWR) in ultra-deepwater depth. Ocean Eng. 197. https://doi.org/10.1016/j.oceaneng.2019.106902

Lenci S, Callegari M. Simple analytical models for the J-lay problem. Acta Mech. 2005;178:23–39. https://doi.org/10.1007/s00707-005-0239-x.

Li CK, Liu YC, Yi P, et al. Mechanical calculation and scheme analysis of the sinking process of offshore pipelines. China Pet Mach. 2014;42(5):101–6 (**in Chinese**).

Liu Xu, Ai ZJ, Qi JC, et al. Mechanics analysis of pipe lifting in horizontal directional drilling. J Nat Gas Sci Eng. 2016;31:272–82. https://doi.org/10.1016/j.jngse.2016.03.016.

Lun GD, Liu YC, Yi P, et al. Impacts of ocean current and seabed friction on the picking up and laying down processes of oil and gas pipelines. Pet Exp Dev. 2013;40(1):111–6 (**in Chinese**).

Xing JZ, Liu CT, Zeng XH. Nonlinear analysis of submarine pipelines during single point lifting. Ocean Eng. 2002;20(3):29–33. https://doi.org/10.16483/j.issn.1005-9865.2002.03.005 (**in Chinese**).

Xiong HR, Li X, Yin H, Chen S. Submarine pipeline lifting analysis. Shipbuild China. 2010;51(1):51–5.

Wang JL, Duan ML, Wang Y, et al. A nonlinear mechanical model for deepwater steel lazy-wave riser transfer process during installation. Appl Ocean Res. 2015;50:217–26. https://doi.org/10.1016/j.apor.2015.02.004.

Zeng XG, Duan ML, Chen JH. Research on several mathematical models of offshore pipe lifting or lowering by one point. Ocean Eng. 2013;31(1):32–7. https://doi.org/10.16483/j.issn.1005-9865.2013.01.002.